Drastic differences between the release kinetics of two highly related porphyrins in liposomal membranes

mTHPP and pTHPP

Kuntsche, Judith; Rajakulendran, Kirishana; Sabriye, Hibo Mohamed Takane; Tawakal, Navidullah; Khandelia, Himanshu; Hakami Zanjani, Ali Asghar

Published in:
Journal of Colloid and Interface Science

DOI:
10.1016/j.jcis.2023.07.152

Publication date:
2023

Document version:
Final published version

Journal of Colloid and Interface Science 651 (2023) 750–759

Contents lists available at ScienceDirect

Journal of Colloid And Interface Science

journal homepage: www.elsevier.com/locate/jcis

Drastic differences between the release kinetics of two highly related porphyrins in liposomal membranes: mTHPP and pTHPP

Judith Kuntsche [a,*], Kirishana Rajakulendran [a], Hibo Mohamed Takane Sabriye [a], Navidullah Tawakal [a], Himanshu Khandelia [a], Ali Asghar Hakami Zanjani [a,*]

[a] Department of Physics, Chemistry and Pharmacy, University of Southern Denmark, Campusvej 55, 5230 Odense, Denmark

HIGHLIGHTS

- Minor structural differences of hydrophobic porphyrins can distinctly influence their release properties from liposomes.
- mTHPP (meta OH) redistributes much slower than pTHPP (para OH) from liposomal membranes.
- Reversed-phase HPLC experiments indicate a higher partition coefficient for mTHPP.
- In MD simulations, mTHPP has a higher tendency for hydrogen bonding, a larger tilt angle and locates deeper in the membrane.
- Both HPLC and MD simulation results support the observed differences in release and redistribution of mTHPP and pTHPP from liposomal membranes.

GRAPHICAL ABSTRACT

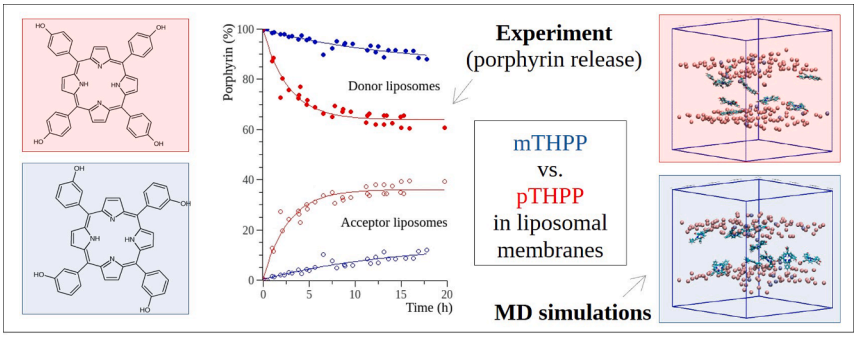

ARTICLE INFO

Keywords:
Liposomes
Porphyrin
Drug release
Partitioning
Molecular dynamics simulation

ABSTRACT

Hypothesis: The release of hydrophobic compounds from liposomal membranes occurs by partitioning and is thus determined by the physicochemical properties (e.g. logP and water solubility) of the drug. We postulate that even minor structural differences, e.g. the position of the phenolic OH-group of the hydrophobic porphyrins mTHPP and pTHPP (*meta* vs. *para* substitution), distinctly affect their partitioning and release behavior from liposomes. *Experiments:* The release and redistribution of mTHPP and pTHPP from lecithin or POPC/POPG liposomes to different acceptor particles (DSPE-mPEG micelles and liposomes) was studied by asymmetrical flow field-flow fractionation to separate donor and acceptor particles. Reversed phase HPLC was applied to detect differences

Abbreviations: AF4, Asymmetrical flow field-flow fractionation; DLPC, Dilinoleoylphosphatidylcholine; DLS, Dynamic light scattering; DPPC, Dipalmitoylphosphatidylcholine; DPPG, Dipalmitoylphosphatidylglycerol; DSPE-mPEG, Distearoylphosphatidylethanolamine-metoxy-polyethylenglycol; HPLC, High-performance liquid chromatography; LS, Light scattering; MALS, Multi-angle light scattering; MD, Molecular dynamics; mTHPC, *meta*-tetrahydroxyphenyl-chlorin; mTHPP, *meta*-tetrahydroxyphenyl-porphyrin; MWCO, Molecular weight cutoff; PdI, Polydispersity index; POPC, Palmitoyl-oleoyl-phosphatidylcholine; POPG, Palmitoyl-oleoyl-phosphatidylglycerol; pTHPP, *para*-tetrahydroxyphenyl-porphyrin; RDF, Radial distribution function; VMD, Visual molecular dynamics; VWD, Variable wavelength detector.

* Corresponding authors.
E-mail addresses: kuntsche@sdu.dk (J. Kuntsche), zanjani@sdu.dk (A.A. Hakami Zanjani).

https://doi.org/10.1016/j.jcis.2023.07.152
Received 26 April 2023; Received in revised form 14 July 2023; Accepted 24 July 2023
Available online 25 July 2023

in partitioning. Molecular dynamics (MD) simulations were carried out to obtain molecular insight in the different behavior of the two compounds inside a lipid bilayer.
Findings: Despite the minor differences in chemical structure, mTHPP is more hydrophobic and redistributes much slower to both acceptor phases than pTHPP. MD simulations indicate that compared to pTHPP, mTHPP makes stronger hydrogen bonds with the lipid head groups, is oriented more parallel to the lipid tails and is embedded slightly deeper in the membrane.

1. Introduction

Drug nanocarriers have been intensively studied during the last decades to improve the clinical efficiency and safety of drugs. The final goal is to obtain a more specific drug action. Using a drug carrier, this can be achieved by, e.g. passive or specific targeting. Macromolecules and nanoparticles can accumulate and be retained in diseased tissues such as tumor tissue due to tissue abnormalities such as increased fenestration of the epithelium (passive targeting by the enhanced permeation and retention effect). By decorating the nanoparticle surface with target-specific ligands, specific targeting becomes possible [1,2]. However, drug nanocarriers may also be used to enable safe administration to the patient, e.g. to solubilize a hydrophobic drug in an aqueous medium. Propofol nanoemulsion, an anesthetic drug, is an example for this purpose [3]. In any case, assessing the drug release properties is of uppermost importance when developing a carrier system for drug delivery.

Liposomes are one of the best known drug nanocarriers and liposomal doxorubicin (Doxil) was the first approved liposomal nanodrug [4]. Liposomes are phospholipid vesicles and can be used as carrier for both hydrophilic (encapsulated in the liposomal aqueous core, e.g. Doxil) and hydrophobic (incorporated in the liposomal membrane, e.g. Visudyne) drugs. Similarly to verteporfin (Visudyne), temoporfin (*meta*-tetrahydroxyphenyl-chlorin, mTHPC) is a second-generation photosensitizer and is approved as Foscan, which is a solution for intravenous injection containing the drug dissolved in a mixture of water-free ethanol and propylene glycol [5]. Temoporfin is practically insoluble in water and has a considerably high logP of around 9 (pub-chem). Due to its poor solubility, there is a risk of drug precipitation at the injection side when injected too rapidly [5]. To circumvent this problem and to potentially improve its biodistribution, a liposomal formulation has been developed among other formulation strategies [6]. Whereas mTHPC is not released into aqueous solutions [7], it redistributes to lipophilic acceptor particles, such as liposomes or serum components [8]. This makes the drug very interesting for both mechanistic studies as well as to establish reliable analytical tools to assess drug release from lipidic carriers. For economic reasons, porphyrins with similar chemical structure and physicochemical properties (water-insolubility, high logP) such as pTHPP (*para*-tetrahydroxyphenyl-porphyrin) have been used as model compounds for temoporfin (mTHPC) [9]. The differences between both compounds is the position of the phenolic OH-groups and the missing double bond in the chlorin structure (Fig. 1). Although results cannot directly be compared due to the different experimental setups, it appears from the different studies that pTHPP redistributes somewhat faster than mTHPC from liposomal carriers [8,9,10,11]. This indicates that even minor structural differences may affect drug release kinetics.

The aim of the present study was to elaborate the effect of the position of the phenolic OH-groups in porphyrin molecules (*meta*- vs. *para*-position, mTHPP and pTHPP) on release kinetics, partitioning and accommodation of the molecules in the liposomal membrane in a combined experimental and computational simulation approach.

The ultimate goal when designing a drug carrier is to control its biodistribution and release of its cargo in the target tissue. For a drug incorporated in the liposomal aqueous core, the membrane presents a release barrier and drug release can be controlled by adjustment of the membrane properties (fluidity and permeability). Indeed, insufficient drug release is often a challenge in this case and liposomal formulations responding to a trigger (e.g. temperature, pH) to release their cargo have been intensively studied [12,13]. In the case of hydrophobic drugs incorporated in the liposomal membrane, such a barrier does not exist and drug release occurs by partitioning [14]. Typical lipophilic drugs with moderate partition coefficients (logP between 3 and 5) and a certain water solubility will more or less instantly partition into the water phase upon dilution and may then redistribute into other lipophilic domains such as lipoproteins in serum. In the case of highly hydrophobic, water-insoluble compounds, as the porphyrins used in this study, partitioning into the water phase will not occur and a lipophilic acceptor phase is necessary for drug redistribution. Therefore, a suitable separation method is needed to separate donor (porphyrin-loaded liposomes) and acceptor particles. In this study, a recently established setup using asymmetrical flow field-flow fractionation (AF4) with inline detection (absorbance) has been applied [15]. In AF4, the sample is separated in a thin channel by applying a cross-flow perpendicularly to the channel flow (Fig. 2) [16]. A semipermeable membrane (often called accumulation wall) is placed in the bottom of the channel allowing excess solvent to pass and to establish a cross-flow. Due to the laminar flow in the channel, flow velocity will increase with increasing distance from the membrane. The cross-flow forces the particles in the channel downward to the accumulation wall but particles will also move by diffusion in all directions. Smaller particles with higher diffusion velocity will accumulate at a higher distance above the membrane than

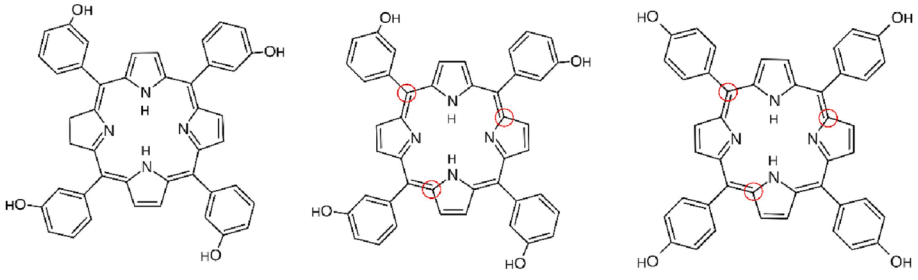

Fig. 1. Chemical structure of mTHPC (temoporfin), mTHPP and pTHPP. Note the differences in number of double bonds in the chlorin (mTHPC) and porphyrin (mTHPP and pTHPP) structure. The C-atoms used to define the porphyrin plane in the MD simulations are highlighted by red circles.

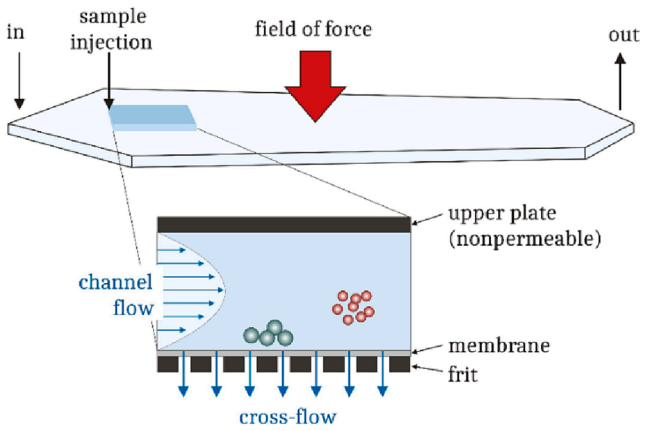

Fig. 2. Schematic presentation of the AF4 separation principle. See text for details. Adjusted after Yohannes et al. 2011 [16].

bigger particles. As a result, smaller particles elute faster than larger particles.

An advantage of AF4 compared to complementary separation techniques such as size exclusion chromatography is the broad separation range and versatility in separation conditions which can be adjusted to the samples to be analyzed. This was an important issue in this study where both very small (micelles, diameter around 15 nm) and rather large (liposomes, diameter around 300 nm) acceptor particles had to be separated from the porphyrin-loaded donor liposomes (size around 100 nm).

The orientation and location of a molecule in the liposomal membrane are considered to play an important role with respect to its release [14]. Molecular dynamics (MD) simulation is a powerful tool to address such questions. The increasing availability of computational capacity over the last decades resulted in the rapid growth of research and applications of MD simulations in life science and pharmaceutical research [17]. Lipid membranes play a crucial role for cell function, drug absorption and last but not least for the performance as drug carrier (liposomes). Consequently, a lot of work has been done to simulate these rather complex systems [18]. Recently, MD simulations have been carried out with pTHPP in different liposomal membranes [19]. An interesting result of this study is that even minor differences in the membrane composition (one or two double bonds in the fatty acid chains in POPC and DLPC, respectively) affected the location of pTHPP [19]. In the present study, MD simulations have been applied to elucidate potential differences in the molecular orientation and dynamical behavior of between mTHPP and pTHPP in lipid membranes.

2. Materials and methods

2.1. Materials

Soybean lecithin (Lipoid E80S) and distearoyl-phosphatidy lethanolamine-N-[methoxy(polyethylene glycol)-2000], sodium salt (DSPE-mPEG) were obtained from Lipoid, palmitoyl-oleoyl-phosphatidylcholine (POPC) and palmitoyl-oleoyl-phosphatidylg lycerol, sodium salt (POPG) from Avanti Polar Lipids. Trizma preset crystals pH 7.4, sodium azide and *para*-tetrahydroxyphenyl-porphyrin (pTHPP, purity 95 %) were purchased from Sigma Aldrich, chloroform, methanol and acetonitrile (all HPLC grade) from VWR and *meta*-tetrahydroxyphenyl-porphyrin (mTHPP, purity $\geq$ 98 %) from PorphyChem. Purified water was obtained from a laboratory water purification system (Milli-Q Advantage A10, Millipore).

2.2. Preparation of the formulations

2.2.1. Donor liposomes

The liposomes were composed of 20 mg/ml phospholipid (Lipoid E80S or POPC/POPG 9:1w/w) in 10 mM Tris buffer pH 7.4 preserved with 0.02 % w/w sodium azide and loaded with 1 mg/ml porphyrin (pTHPP or mTHPP) corresponding to about 5 mol % related to the lipid. Control samples were prepared without adding porphyrin. Two batches of lecithin donor liposomes (both liposomes loaded with porphyrin and the control formulation without porphyrin) were prepared independently.

The lipids and porphyrins were dissolved in chloroform and methanol, respectively, and the required volumes were mixed. The organic solvents were removed using a rotary evaporator (Laborota 4000 efficient, Heidolph) at 50 °C and 200–400 mbar followed by drying the lipid film for 1 h at 30–50 mbar at the same temperature. The lipid film was then dispersed in Tris buffer by gentle shaking at room temperature. The crude liposome suspensions were extruded at least 21 times each through membranes with decreasing pore size (400, 200, 100 and 50 nm, LiposoFast, Avestin) and stored at 4–8 °C under light protection.

2.2.2. Acceptor liposomes

Large acceptor liposomes were prepared by the thin-lipid film method as described in 2.2.1. but without addition of porphyrin and with a lipid concentration of 50 mg/ml. The crude liposome suspension was extruded 9 to 21 times through a membrane with a pore size of 400 nm and diluted to 1 mg/ml lipid with Tris buffer. 50 ml of the diluted suspension was centrifuged until a pellet was obtained (2–6 h, 4400 rpm, Centrifuge 5702 RH, Eppendorf). The pellet was washed by redispersing it in Tris buffer and repeating centrifugation. The pellet was finally dispersed in a suitable volume of Tris buffer and the lipid concentration was determined by high-performance thin-layer chromatography [20]. The lipid concentration was adjusted to 2 mg/ml with Tris buffer and the samples were stored at 4–8 °C under light protection.

2.2.3. Acceptor micelles

100 mg DSPE-mPEG were dissolved in 5 ml 10 mM Tris buffer pH 7.4 preserved with 0.02 % w/w sodium azide. The sample was heated to 70 °C for 30 min and then stored at room temperature.

2.3. Dynamic light scattering (DLS)

The average vesicle size was determined by dynamic light scattering (DelsaMax Pro, Beckman-Coulter). The diluted samples (0.1 mg/ml lipid in 10 mM Tris buffer) were measured 6 times over 10–30 s at 20 °C. The z-average diameter and polydispersity index were determined by the instruments cumulant analysis (DelsaMax software version 1.0.1.6, Beckman-Coulter).

2.4. UV/Vis spectroscopy

100 µl liposome suspension were dissolved in 10 ml methanol in a volumetric flask and absorbance was measured at 512 nm (mTHPP) or 516 nm (pTHPP) using methanol as blank. Calibration curves were established by measuring the absorbance of a dilution series of stock porphyrin solutions with known concentration resulting in calibration constants of 0.026 ml μg^{-1} cm^{-1} (mTHPP) and 0.021 ml μg^{-1} cm^{-1} (pTHPP). Liposomes without porphyrin were measured to exclude any interference of the lipid and sample preparation. All determinations were done in triplicate.

2.5. High-performance liquid chromatography (HPLC)

Differences in the partition behavior of mTHPP and pTHPP were investigated by reversed-phase HPLC (degasser, binary pump, autosampler, diode-array detector set to 420 nm, all from Agilent 1100 series). 20 µl of solutions in methanol containing 0.05 mg/ml mTHPP or 0.01 mg/ml pTHPP or both were injected into the column (Kinetex 5 µm EVO C18, length 15 cm, diameter 4.6 mm; Phenomenex). Methanol: water 85:15 v/v was used as mobile phase and the flow rate was set to 1 ml/min.

2.6. Asymmetrical flow field-flow fractionation (AF4)

The AF4 instrument (Eclipse 3^{+}, Wyatt) was connected to an Agilent chromatographic system (degasser, isocratic pump, thermostatted autosampler, variable wavelength detector (VWD) set to 420 nm, Agilent 1200 series), a multi-angle light scattering (MALS, DAWN Heleos II, Wyatt) and differential refractive index (dRI, Optilab rEX, Wyatt) detector. The autosampler was set to 37 °C and supplemented with a magnetic stirrer underneath the sample holder. The AF4 channel was equipped with a trapezoidal-shaped spacer (length 265 mm, largest width 21 mm, height 350 µm) and a membrane of regenerated cellulose or polyethersulfone (both with 10 kDa MWCO, Wyatt). Samples (typically 20 µl) were injected with 0.2 ml/min, focused (focus flow 2 ml/min) for 8 min and then eluted at constant channel flow of 1 ml/min. To separate micelles and small donor liposomes, a constant cross-flow of 1 ml/min was applied over 10 min followed by elution without applied cross-flow to elute the liposomes. Small donor and large acceptor liposomes were fractionized by applying a cross-flow gradient from 1 ml/min to 0.15 ml/min over 5 min, keeping the cross-flow constant at 0.15 ml/min for 15 min followed by elution without applied cross-flow. 10 mM Tris buffer pH 7.4 preserved with 0.02 % w/w sodium azide was used as carrier liquid and for sample dilution.

Data was analyzed with the Astra software (Wyatt). Particle sizes were calculated by analyzing the angular light scattering profile applying the coated sphere model (refractive index of 1.33 and 1.45 for the aqueous core and lipid membrane, respectively, and assuming a membrane thickness 4.5 nm). For porphyrin quantification in the sample fractions, the VWD signals at 420 nm were integrated after baseline correction and peak determination. Control samples (without porphyrin) were used to correct scattering effects [15]. Calibration constants were determined by injecting different amounts of liposomes loaded with mTHPP and pTHPP, respectively, directly into the detector and were 0.60 ml μg^{-1} cm^{-1} (mTHPP) and 0.40 ml μg^{-1} cm^{-1} (pTHPP). Note that different wavelengths have been used to quantify the porphyrins in the liposome suspensions (cf. 2.4.) and the transfer studies resulting in different calibration constants. The porphyrins have very characteristic UV/Vis spectra with the highest absorbance around 420 nm (Sorbet band) followed by several minor absorption peaks at higher wavelengths (Q band region) [21].

2.7. Redistribution studies

500 µl donor liposomes (diluted to 2 mg/ml lipid and 0.1 mg/ml porphyrin) were mixed with 500 µl acceptor micelles or acceptor liposomes (both diluted to 2 mg/ml) and kept at 37 °C under magnetic stirring. 20 µl of the incubation sample, corresponding to the injection of 40 µg total lipid and 1 µg porphyrin, were immediately submitted to AF4 (cf. 2.6.) and subsequently injected over a period of time for up to about 20 h. Results are presented as percentage in the donor and acceptor fraction related to the total determined amount. Recoveries were calculated by comparing the total detected amount of porphyrin to the theoretical porphyrin amount of the injected sample. Recoveries were > 85 %, but in most cases > 90 %. As controls, a mixture of small liposomes without porphyrin and the acceptor particles (micelles or large liposomes) as well as donor and acceptor particles separately were analyzed.

The experimental data were fitted (SciDAVis version 1.26) using the exponential decay function $y = y_{equ} + Ae^{-kt}$ with y the actual amount of porphyrin (%), y_{equ} the porphyrin amount in equilibrium (plateau; %), A the amplitude (%), k the rate constant (h^{-1}) and t the time (h). The half-life $t_{1/2}$ is calculated by $t_{1/2} = \ln 2/k$.

2.8. MD simulations

Bilayer systems were created using the CHARMM-GUI program [22] at a fixed POPC:POPG ratio (180:20 molecules) in a water phase containing 150 mM KCl. 9 porphyrin molecules were distributed randomly into the lipid bilayer. All simulations were performed using the Gromacs2020.3 software [23], using the OPLS all-atom force field [24], and TIP3P water model [25]. For each system, 4 replicas were simulated for 1000 ns at 310 K (Nosé-Hoover thermostat [26,27]) and 1 atm (Parrinello-Rahman barostat [28]). In all simulations, the cutoff distance for van-der-Waals interactions was set to 1.0 nm. The Particle Mesh Ewald (PME) [29] summations for long-range electrostatic interactions with 0.12 nm grid spacing and 1.0 nm cutoff distance for real space summation was applied. The force field for mTHPP and pTHPP was kindly provided by late Dr. Tomasz Rog. All calculations were performed for the last 500 ns of the simulation where the coordinates of the atoms were saved in intervals of 0.1 ns. Images of the systems were prepared using the VMD molecular visualization software [30].

To estimate the orientation of the porphyrin molecules in the membrane, the distribution of the angle between the vector perpendicular to the porphyrin plane and the membrane normal was calculated. For this, the porphyrin plane was defined by the plane passing through three hybridized carbon atoms of the porphyrin structure as indicated in Fig. 1. The three-dimensional radial distribution functions (RDF) were determined by calculation of the ratio of the average local number density of the phenolic OH-groups of the porphyrins at a distance r from the phosphorous atoms to the bulk density of the phenolic OH-groups of the porphyrins. The depth of the porphyrin molecules in the membrane was determined by analyzing the partial density of the porphyrin molecules along the membrane normal. As reference, the density of the phosphorous atoms in the phospholipids head group was also calculated. To increase clarity, data were normalized to 1 by dividing each value by the maximum value.

3. Results and discussion

3.1. Characterization of the formulations

To enable studies of drug redistribution between donor and acceptor particles, both fractions must be separated for drug quantification. In AF4, separation is based on hydrodynamic size and to study drug redistribution between different colloidal fractions, donor and acceptor particles must have distinctly different sizes preferably without overlap in their size distributions. Small liposomes with diameters around or below 100 nm were used as donor particles in all experiments (Table 1). As acceptor phases, DSPE-mPEG micelles or large liposomes with the same lipid composition as the donor liposomes were used. The micelles had an average hydrodynamic size of around 15 nm (DLS: z-average 14.5 ± 0.5 nm, PDI 0.239 ± 0.022, n = 6). Due to the very low critical micelle concentration of DSPE-mPEG (about 5 µM in 150 mM NaCl [31]), the micelles were stable during AF4 runs. Suspensions of large acceptor liposomes were prepared by slow extrusion followed by centrifugation to eliminate the fraction of small vesicles which would overlap in size with the donor liposomes. After centrifugation, the acceptor liposomes had average sizes between 300 and 400 nm.

Table 1
Characteristics of the prepared donor liposomes. Liposomes were prepared from purified egg lecithin (E80S) or POPC/POPG 9:1 w/w (POPC/PG) in 10 mM Tris buffer pH 7.4 at a lipid concentration of 20 mg/ml. All formulations were preserved with 0.02 % sodium azide.

Sample code	DLS (n = 6)		AF4/MALS				c_{THPP} (mg/ml) (n = 3)
	Diameter (nm)	PdI	Distribution moments* (nm)			Dw (nm) (n = 3)	
			D10	D50	D90		
E80S_D	89.2 ± 0.4	0.089 ± 0.010	64	86	114	103 ± 1	—
	91.6 ± 0.1	0.082 ± 0.016	84	94	113	91 ± 4	—
E80S_mTHPP	95.1 ± 0.8	0.078 ± 0.024	88	97	124	97 ± 4	1.21 ± 0.02
	99.3 ± 0.6	0.100 ± 0.010	66	96	128	114 ± 3	0.82 ± 0.01
E80S_pTHPP	88.7 ± 1.1	0.064 ± 0.030	82	90	110	90 ± 2	0.90 ± 0.03
	81.4 ± 0.5	0.074 ± 0.014	48	70	98	88 ± 5	0.97 ± 0.01
POPC/PG_D	101.9 ± 1.0	0.064 ± 0.028	98	116	130	106 ± 2	—
POPC/PG_mTHPP	87.8 ± 0.7	0.149 ± 0.017	77	93	107	89 ± 2	1.32 ± 0.02
POPC/PG_pTHPP	71.7 ± 0.58	0.072 ± 0.026	64	74	93	75 ± 1	0.88 ± 0.06

* Distribution moments are given for one representative analysis from AF4/MALS. D10, D50 and D90 are the diameters at 10 %, 50 % and 90 % of the cumulative size distribution. The D10 diameter, for example, indicates that 10 % or the particles are smaller than this value and 90 % are bigger.

3.2. Redistribution studies

In Fig. 3, representative AF4 elution profiles for the redistribution experiments are plotted together with the applied cross-flow. The first step in all separations is a focus step (the first 10 min of the experiments) and sample injection. During focusing, the solvent is entering the channel from both inlet and outlet and focuses the injected sample to a band just behind the injection port. After complete focusing, the sample is eluted by applying suitable cross-flow conditions. Fig. 3**A** shows the separation of micelles (acceptor) and liposomes (donor). According to the AF4 separation principle, the micelles (diameter around 15 nm) elute before the distinctly larger liposomes (diameter around 100 nm). Due to the distinct difference in size, both fractions could be baseline-separated. After complete elution of the micelles, the cross-flow was set to zero to rapidly elute all the liposomes. Light scattering (LS) intensity strongly depends on size and that is the reason for the very weak LS signal (red line) in the micelle fraction. The VWD signals (extinction) are plotted for the 1st (closed blue line) and 10th (dotted blue line) injection of the same incubation sample. The increasing VWD signal in the micelle fraction and the correspondingly declining VWD signal in the liposome fraction reflects the redistribution of the porphyrin (here pTHPP) from the donor liposomes to the micelles.

A similar elution profile is shown in Fig. 3**B** for the experiments with large liposomes as acceptor phase. In this case, the donor liposomes (diameter around 100 nm) elute before the large acceptor liposomes (diameter around 300–400 nm). In contrast to micelles, liposome suspensions are not monodisperse and complete baseline separation could not be reached in these experiments. Moreover, a cross-flow gradient had to be applied to allow elution of the smaller donor liposomes while keeping the larger acceptor liposomes retained in channel. This way, the donor liposomes were fractionized in size and thus eluted over a longer period of time. The fraction of large liposomes was then eluted by setting the cross-flow to zero. Whereas light scattering effects in the VWD signals (extinction) of micelles and small liposomes were negligible, these had to be considered and corrected for in the fraction of large acceptor liposomes. In fact, the VWD signal of the acceptor liposomes in the 1st injection is actually mostly due to light scattering (Fig. 3**B**). However, all separations were well reproducible and porphyrin amounts could accurately be measured in both the donor and acceptor fraction.

The results of the redistribution studies are summarized in Fig. 4. In all experiments, mTHPP transferred much slower to the acceptor phase than pTHPP. Redistribution to micelles was much faster (Fig. 4**A**) than to

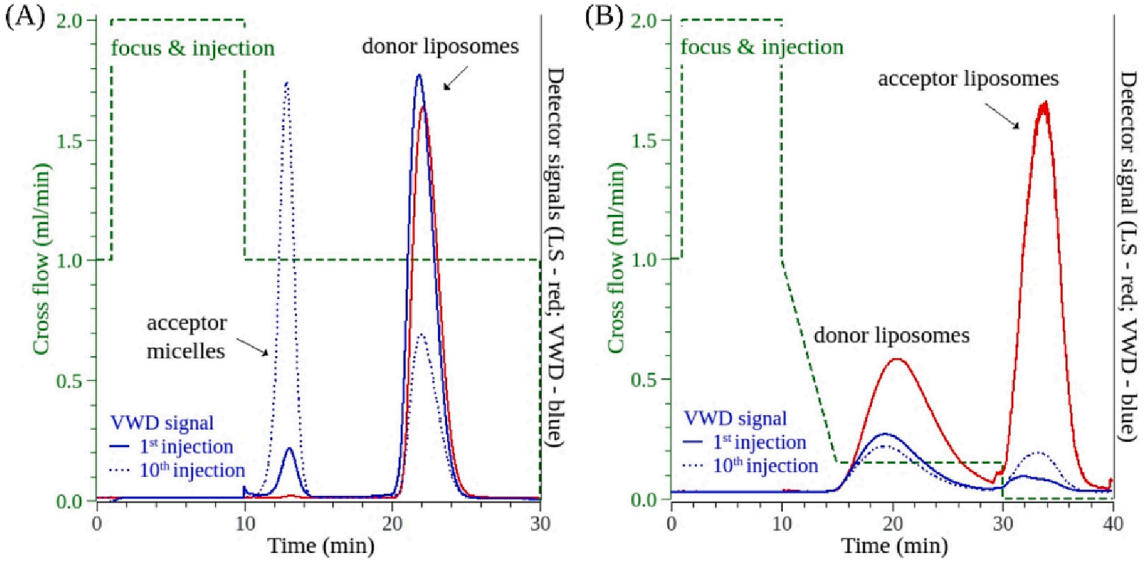

Fig. 3. AF4 analysis of the incubation mixtures using DSPE-mPEG micelles (A) or large E80S liposomes (B) as acceptor phase and pTHPP-loaded E80S liposomes as donor phase (A, B). The elution profiles (light scattering signals at 90°/red lines and VWD signals/blue lines) are shown together with the applied cross-flow conditions (green dashed lines). To illustrate pTHPP redistribution, VWD signals are shown for the first (closed line) and tenth (dotted line) injection of the same incubation sample. Samples were incubated directly in the autosampler at 37 °C under magnetic stirring and subsequently submitted to AF4 analysis. (For interpretation of the references to colour in this figure legend, the reader is referred to the web version of this article.)

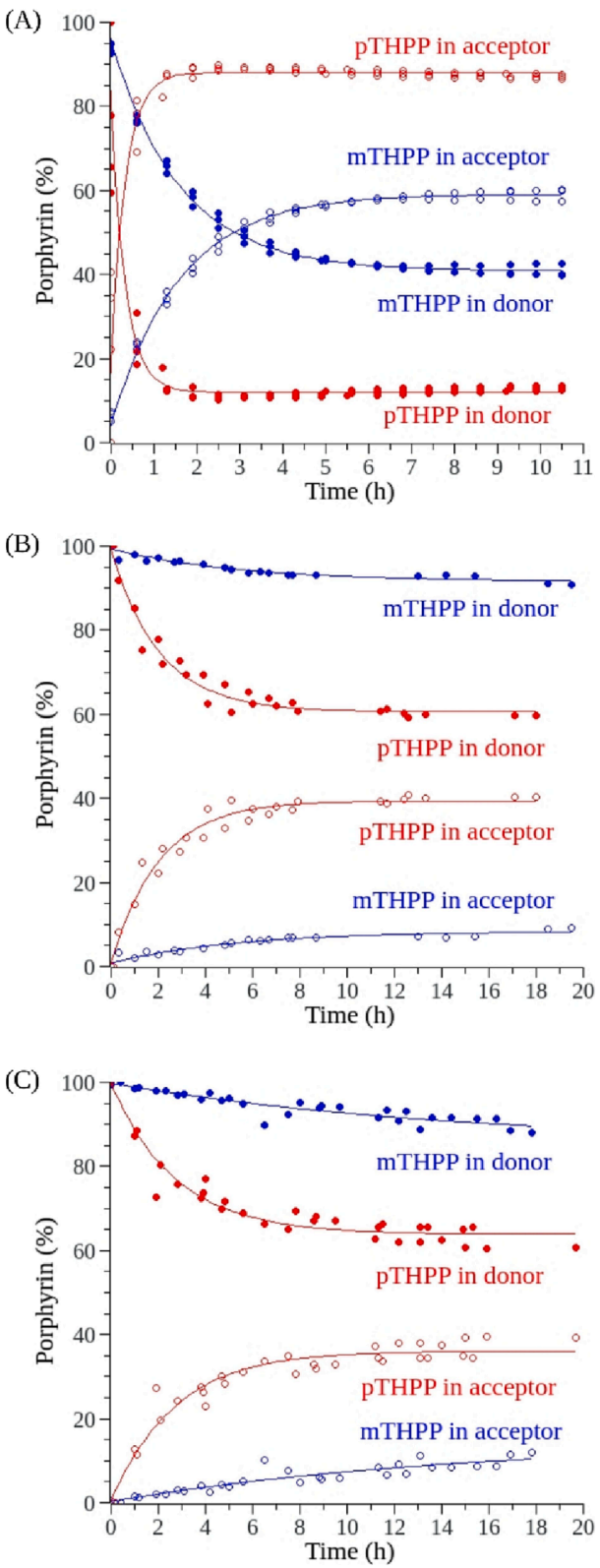

Fig. 4. Redistribution of mTHPP (blue) and pTHPP (red) from liposomes to micelles (A) or to large liposomes (B, C). Liposomes were prepared from egg lecithin (A, B) or POPC/POPG (C). Equal volumes of donor and acceptor dispersions (both 2 mg/ml lipid) were mixed at a total nominal lipid concentration of 2 mg/ml. Samples were incubated at 37 °C under stirring and subsequently submitted to AF4 using 2–3 independently prepared incubation mixtures. Dots represent the experimental data points and lines the first-order exponential fits. (For interpretation of the references to colour in this figure legend, the reader is referred to the web version of this article.)

liposomes (Fig. 4**B**) for both porphyrins. The data could be fitted using an 1st order exponential decay function and the fit values are given in Table 2.

The faster redistribution to the micelles can be explained by the much smaller size of the micelles (15 nm) compared to the acceptor liposomes (300–400 nm) resulting in a higher collision rate in the samples with micelles as acceptor phase. Interestingly, pTHPP accumulated in the micelles to a much greater extent (about 90 %) than mTHPP (about 60 %) pointing to differences in partitioning behavior. However, in both cases the majority of the porphyrin molecules is in the micelle fraction indicating a higher affinity to the micelles than to the liposomal membrane. This is supported by results of the recent MD simulation study exploring pegylated liposomes where the PEG corona of the liposomes has been detected as one preferred region for pTHPP in addition to the liposomal membrane [19].

When using large liposomes as acceptor phase, equilibrium was not reached in the time window used in this study for mTHPP and only a remarkably low amount (about 7 %) was found in the acceptor liposomes after incubation for about 14 h in contrast to about 40 % for pTHPP. Generally, an equal distribution can be expected in equilibrium in these experiments as the chemical composition and concentration is the same for both donor and acceptor liposomes. The reason for the plateau values not reaching 50 % may be due to the fact, that the acceptor liposomes are not all unilamellar [15] and redistribution between the internal liposomal membranes may not be complete and kinetics may be different.

To facilitate comparison of experimental results with the simulations, redistribution experiments were also carried out using liposomes composed of pure synthetic lipids (POPC/POPG 9:1 w/w), e.g. with comparable bilayer composition as applied in the simulation studies. The redistribution of the porphyrins from the POPC/POPG liposomes was rather similar to that obtained with lecithin liposomes (Fig. 4**B** and **C**).

3.3. *mTHPP and pTHPP partitioning*

Direct experimental determination of partition coefficients of the porphyrins is not feasible due to their insolubility in water. Reversed-phase HPLC can be used to determine octanol/water partition coefficients in the range from 0 to 6 [32] but also just to detect differences in the partition behavior even if logP values are not calculated. Indeed, mTHPP was more retained in the column (retention time 4.5 min) indicating stronger affinity to the hydrophobic stationary phase than pTHPP (retention time 3.6 min, Fig. 5). These results are in good agreement with a previous study applying a different RP-HPLC method [33] and may explain the slower redistribution of mTHPP in the transfer experiments.

3.4. *MD simulations*

To get insight into the behavior of the porphyrins in liposomal bilayers and to facilitate a better understanding of the experimental results, MD simulations were carried out. Representative images of the simulation and the mean tilt angle of mTHPP (bottom) and pTHPP (top) together with the angle distributions in the POPC/POPG bilayers are shown in Fig. 6.

The higher the angle the more the molecules become aligned parallel to the lipid chains and at an angle of 0°, the molecules would arrange perpendicularly to the lipid chains. Both porphyrins are tilted with respect to the membrane normal with mean angles of 36.1° and 26.1° for mTHPP and pTHPP, respectively. The preferred angle (maximum of distribution) is 30.4° for mTHPP and 17.7° for pTHPP. It is worth to note that the angle distribution is distinctly broader for the mTHPP molecules with tilt angles up to 70° (Fig. 6). This indicates a higher degree of orientational freedom for the mTHPP molecule in the lipid membrane as well as a higher probability of an orientation more aligned with the lipid

Table 2
Values obtained by fitting the experimental data (release of porphyrin from donor liposomes) with a first-order exponential decay function: $y = y_{equ} + Ae^{-kt}$.

	Micelles as acceptor phase		Liposomes as acceptor phase			
	mTHPP	pTHPP	mTHPP		pTHPP	
			E80S	POPC/PG	E80S	POPC/PG
Plateau value y_{equ} (%)	40.9 ± 0.3	12.0 ± 0.9	91.6 ± 0.5	85.3 ± 4.3	60.6 ± 0.7	63.9 ± 0.7
Rate constant k (h^{-1})	0.63 ± 0.01	3.03 ± 4.39*	0.19 ± 0.01*	0.07 ± 0.00*	0.49 ± 0.01	0.37 ± 0.01
Half-life $t_{1/2}$ (h)	1.1	0.2*	3.6*	9.9*	1.4	1.9
Fit constant R^2	0.999	0.964	0.999	0.999	0.964	0.999

* These values should be interpreted with care due to the very fast transfer (pTHPP to micelles, only a few data points in the region of largest change) or very low extent of transfer (mTHPP to liposomes).

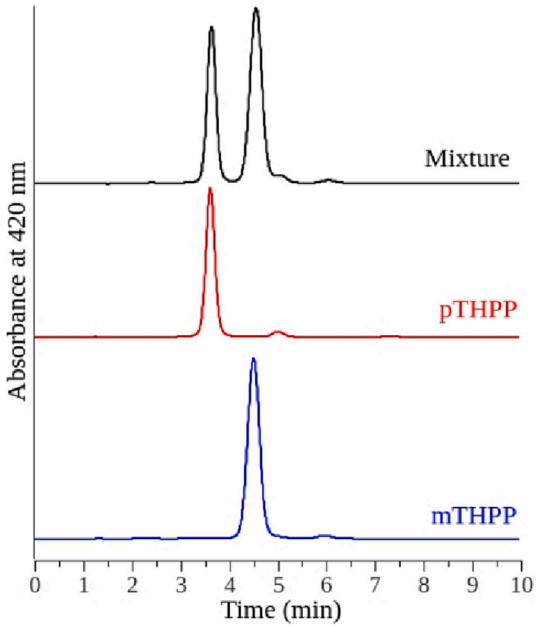

Fig. 5. Reversed-phase HPLC chromatograms of solutions of mTHPP, pTHPP and a mixture of both in methanol using an C18 RP-column as stationary and methanol/water 85:15 v/v as mobile phase.

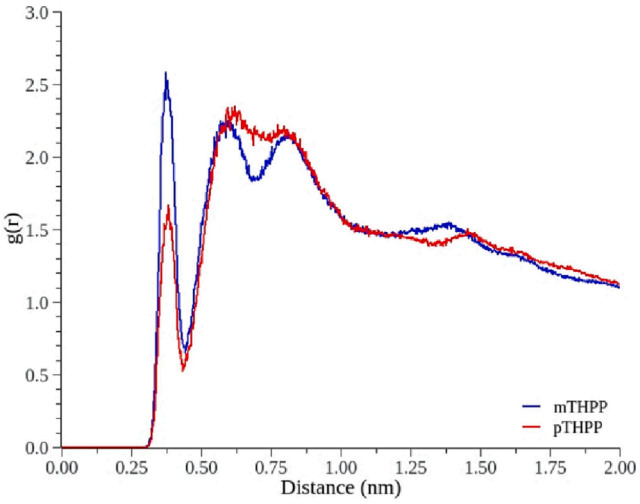

Fig. 7. Radial distribution functions describing how the density of the phenolic OH-groups of the porphyrins varies as a function of the distance from the phosphorous atoms.

chains compared to pTHPP.

The radial distribution functions in Fig. 7 depict a measure of the probability of finding the OH-groups of the porphyrins at a distance of *r* away from the phosphorous atoms. It should be kept in mind that each porphyrin molecule contributes with 4 OH-groups which all have different distances due the tilt angle of the porphyrin molecules in the membrane. The defined sharp maxima at a distance of around 0.37 nm from the phosphorous atom indicate rather distinct electrostatic interactions by hydrogen bonding with a distinctly higher tendency of hydrogen bonding for mTHPP (higher maximum). The higher tendency of hydrogen bonding with the phospholipid head groups appears to result in more defined orientations of mTHPP as visible by the rather distinct second and third maxima (Fig. 7).

The depth profile of the porphyrins in the membrane is shown in Fig. 8 where the phosphorous atoms of the POPC head group are shown as reference. Generally, the depth profiles are rather similar for both porphyrins with the density distribution of mTHPP slightly broader towards the membrane center. This might be due to the different

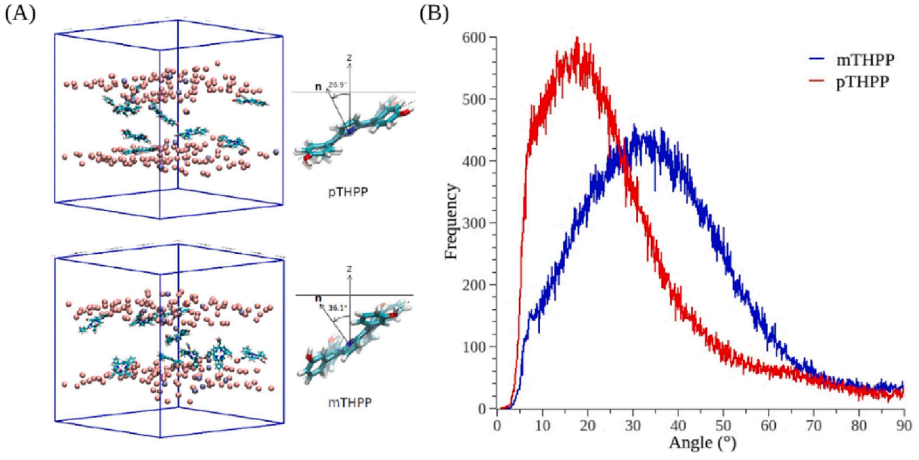

Fig. 6. Representative images of the distribution of pTHPP (up) and mTHPP (down) in the lipid bilayer (A). Phosphorous atoms of the POPC and POPG lipids are shown as pink and ice blue spheres, respectively. Water and lipid molecules are not shown for clarity. The mean values of the angles between porphyrin normal vector (n) and membrane normal (z axis) are illustrated in the right images in (A). Distributions of the angle between the vector perpendicular to the porphyrin plane and the membrane bilayer normal in the mTHPP (blue) and pTHPP system (red) are shown in (B). (For interpretation of the references to colour in this figure legend, the reader is referred to the web version of this article.)

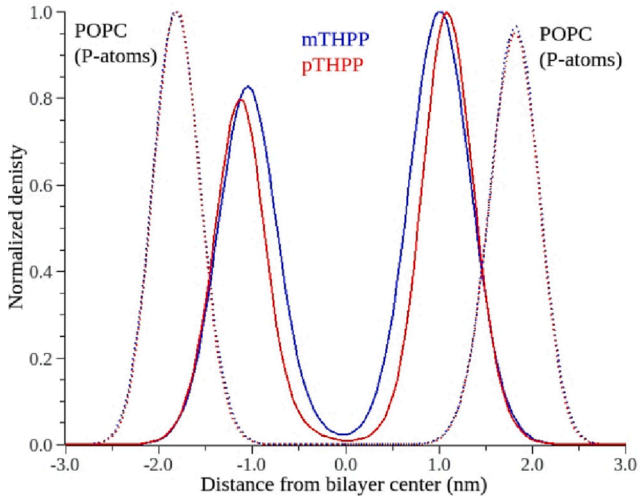

Fig. 8. Normalized density of the phosphorous atoms of the lipids (dashed lines) and porphyrin molecules (closed lines) in the mTHPP (blue) and pTHPP (red) system. Each data point was divided by the maximum value (normalization to 1) to increase clarity. (For interpretation of the references to colour in this figure legend, the reader is referred to the web version of this article.)

arrangements of the porphyrins in the membrane (higher tilt angle for the mTHPP molecules). The center of the membrane is generally not a preferred location for none of the two porphyrins (minimum in the density curve in the center of the membrane, Fig. 8) indicating that the molecules will not easily flip-flop between the membrane leaflets.

In a recent study, the location and orientation of pTHPP molecules in POPC and DLPC membranes together with the effect of pegylation has been investigated by MD simulations [19]. Similarly as found in the present study, there was a minimum in the density profile of the porphyrin in the membrane center and a high energy barrier was calculated for pTHPP to translocate from one to the other leaflet [19]. However, in addition to the location close to the phospholipid head groups, a second location deeper in the membrane with an orientation more or less perpendicular to the fatty acid chains has also been detected in the POPC system in the previous study. These deviations may be due to differences in the setup of the model systems (4 molecules placed outside the membrane in the previous vs. 9 randomly placed inside the membrane in our study) as well as differences in the membrane composition (POPC vs. POPC/POPG). The addition of the negatively charged POPG in the membrane system in our study may result in increased electrostatic interactions of the phenolic OH-groups of the porphyrin with the phospholipid head groups and thus favor a location closer to the phospholipid head groups. Interestingly, increasing fatty acid unsaturation (DLPC membranes) resulted in only one preferred location of pTHPP deeper in the membrane [19].

4. Conclusions

Water-insoluble hydrophobic compounds such as temoporfin, mTHPP and pTHPP will redistribute from liposomal membranes upon collision of the donor and acceptor particles [14]. Indeed, in absence of a lipophilic acceptor phase, the porphyrins remain in the liposomal membranes and do not diffuse out into the water phase [7,34]. A mathematical model describing the release kinetics of hydrophobic drugs from liposomal membranes has been developed [35] and applied for liposomal formulations of temoporfin (mTHPC) [8,11]. For the collision mechanism, the major determinant for the redistribution rate for a given compound will be the collision rate of the particles, thus size and concentration [8,9]. This effect is also evident in the present study with a much faster redistribution of both porphyrins when DSPE-mPEG micelles have been used as acceptor phase. However, the models do not account for differences in the physicochemical properties of the drugs and to understand the observed differences in the transfer kinetics for both porphyrins, partitioning - or more accurately the chemical potentials - needs to be taken into account [36].

Generally, donor and acceptor particles will not come in direct contact upon collision, e.g., there is no fusion, and the drug must still diffuse over a certain water layer to reach the lipid domain of the acceptor particle. Lipid membranes are dynamic systems and it is worth to note the rather broad range of the positions of the POPC phosphorous atoms (about 1.5 nm in the density profile, Fig. 8), which is a considerable distance assuming an average membrane thickness of about 4.5 nm. This way, the porphyrin molecules located close the phospholipid head groups will, at least for very short periods of time, be exposed to the surrounding water phase and may escape if a lipidic acceptor particle is available. Although the density profiles for both porphyrins in this region (overlap of density profiles of the phosphorous atoms and porphyrins, Fig. 8) are rather similar, simulations were carried out in equilibrium. From the simulations, the most distinct differences between both porphyrins are the interactions with the POPC head group (hydrogen bonding) and the arrangement with respect to the lipid chains (tilt angle). The stronger tendency of hydrogen bonding of mTHPP may result in a hindrance or higher energetic barrier for mTHPP to escape to the surrounding water phase compared to pTHPP. Moreover, the larger tilt angle of mTHPP in the POPC/POPG membrane and thus better alignment with the fatty acid chains may play an important role. It is hypothesized that the diffusion path length into the water phase may be different for both porphyrins where pTHPP may be able to diffuse over somewhat longer distances (albeit not completely diffusing into the water phase). This could also explain why pTHPP redistributes within the large acceptor liposomes (which are not unilamellar) reaching nearly equal distribution between donor and acceptor in equilibrium but mTHPP does not (or to a much lower extent). This hypothesis may be supported by the fact that drug release from liposomes to lipidic acceptor phases can be more or less completely suppressed by using a lipophilic prodrug with a suitable lipid anchor [37].

It is well established that porphyrin molecules may self-aggregate [38] which is of clinical relevance in photodynamic therapy [39] but may also facilitate synthesis of porphyrin derivates with new functionalities [40]. The phase segregation which has been observed with increasing mTHPC loads in DPPC/DPPG membranes [41] may be attributed to this effect. In the present study, there was no indication of self-aggregation of the porphyrin molecules in the MD simulations. The experimental data of drug redistribution could be fitted with a simple first-order exponential decay function also indicating the absence of attractive drug-drug interactions in the liposomal membranes [35]. Nevertheless, potential differences in the aggregation tendency of mTHPP and pTHPP will be interesting to explore both to get more information about the effect of the position of the phenolic OH-group on the physicochemical properties and its impact on the release and transfer kinetics of the porphyrins.

In conclusion, despite the position of the phenolic OH-group being the only structural difference between the studied porphyrins, drug release and redistribution kinetics are distinctly different. Both HPLC (higher partition coefficient for mTHPP) and MD simulations (higher tendency of hydrogen bonding with phospholipid head group, larger tilt angle for mTHPP) can explain the much slower redistribution of mTHPP compared to pTHPP, but more work is needed to understand and mathematically describe the process of drug release from the liposomes and transfer to the acceptor particles by collision. Moreover, as pTHPP is a completely symmetric molecule in contrast to mTHPP, where the *meta*-position of the phenolic OH-group together with the rotational freedom of the phenol ring can result in different molecular arrangements, the results appear somewhat surprising. Further work will focus on this issue and explore the processes involved in drug redistribution via collision of donor and acceptor particles on the molecular level.

CRediT authorship contribution statement

Judith Kuntsche: Conceptualization, Methodology, Formal analysis, Validation, Writing – original draft, Writing – review & editing. **Kirishana Rajakulendran:** Investigation, Formal analysis. **Hibo Mohamed Takane Sabriye:** Investigation, Formal analysis. **Navidullah Tawakal:** Investigation, Data curation, Formal analysis. **Himanshu Khandelia:** Conceptualization, Methodology, Data curation, Formal analysis, Writing – review & editing. **Ali Asghar Hakami Zanjani:** Conceptualization, Methodology, Data curation, Formal analysis, Investigation, Writing – review & editing.

Declaration of Competing Interest

The authors declare that they have no known competing financial interests or personal relationships that could have appeared to influence the work reported in this paper.

Data availability

Data will be made available on request.

Acknowledgements

H.K. is supported by a Lundbeckfonden Ascending Investigator grant no. R344-2020-1023. A.A.H.Z. and H.K. are supported by the Novo Nordisk Foundation grant no. NNF18OC0034936. The simulations were performed on the Novo Nordisk Foundation-funded ROBUST Resource for Biomolecular Simulations no. NNF18OC0032608 and the DECI resource Kay based in Ireland at ICHEC with support from the PRACE aisbl.

The authors thank late Dr. Tomasz Ròg for sharing force field parameters for the compounds and Lipoid GmbH for providing lecithin Lipoid E80S and DSPE-mPEG 2000.

References

[1] V.P. Torchilin, in: M. Schäfer-Korting (Ed.), Drug Delivery, Handbook of Experimental Pharmacology, 197, Springer Berlin Heidelberg, Berlin, Heidelberg, 2010, pp. 3–53, https://doi.org/10.1007/978-3-642-00477-3_1.

[2] F. Danhier, To exploit the tumor microenvironment: since the EPR effect fails in the clinic, what is the future of nanomedicine? J. Control. Release 244 (2016) 108–121, https://doi.org/10.1016/j.jconrel.2016.11.015.

[3] D.S. Ward, J. Russell Norton, P.H. Guivarc'h, R.S. Litman, P.L. Bailey, Pharmacodynamics and pharmacokinetics of propofol in a medium-chain triglyceride emulsion, Anesthesiology 97 (2002) 1401–1408, https://doi.org/10.1097/00000542-200212000-00011.

[4] Y. Barenholz Chezy, Doxil® — the first FDA-approved nano-drug: lessons learned, J. Control. Release 160 (2012) 117–134, https://doi.org/10.1016/j.jconrel.2012.03.020.

[5] EMA, Foscan - EPAR Product Information, 2016, https://www.ema.europa.eu/en/medicines/human/EPAR/foscan.

[6] A. Wiehe, M.O. Senge, The photosensitizer temoporfin (mTHPC) – chemical, Preclinical and clinical developments in the last decade, Photochem. Photobiol. (2022), 13730, https://doi.org/10.1111/php.13730.

[7] J. Kuntsche, C. Decker, A. Fahr, Analysis of liposomes using asymmetrical flow field-flow fractionation: separation conditions and drug/lipid recovery, J. Sep. Sci. 35 (2012) 1993–2001, https://doi.org/10.1002/jssc.201200143.

[8] H. Hefesha, S. Loew, X. Liu, S. May, A. Fahr, Transfer mechanism of temoporfin between liposomal membranes, J. Control. Release 150 (2011) 279–286, https://doi.org/10.1016/j.jconrel.2010.09.021.

[9] A.H. Hinna, S. Hupfeld, J. Kuntsche, A. Bauer-Brandl, M. Brandl, Mechanism and kinetics of the loss of poorly soluble drugs from liposomal carriers studied by a novel flow field-flow fractionation-based drug release-/transfer-assay, J. Control. Release 232 (2016) 228–237, https://doi.org/10.1016/j.jconrel.2016.04.031.

[10] A.H. Hinna, S. Hupfeld, J. Kuntsche, M. Brandl, The use of asymmetrical flow field-flow fractionation with on-line detection in the study of drug retention within liposomal nanocarriers and drug transfer kinetics, J. Pharm. Biomed. Anal. 124 (2016) 157–163, https://doi.org/10.1016/j.jpba.2016.02.037.

[11] S. Holzschuh, K. Kaeß, G.V. Bossa, C. Decker, A. Fahr, S. May, Investigations of the influence of liposome composition on vesicle stability and drug transfer in human plasma: a transfer study, J. Liposome Res. 28 (2018) 22–34, https://doi.org/10.1080/08982104.2016.1247101.

[12] L.C. Sebeke, J.D. Castillo Gómez, E. Heijman, P. Rademann, A.C. Simon, S. Ekdawi, S. Vlachakis, D. Toker, B.L. Mink, C. Schubert-Quecke, S.Y. Yeo, P. Schmidt, C. Lucas, S. Brodesser, M. Hossann, L.H. Lindner, H. Grüll, Hyperthermia-induced doxorubicin delivery from thermosensitive liposomes via MR-HIFU in a pig model, J. Control. Release 343 (2022) 798–812, https://doi.org/10.1016/j.jconrel.2022.02.003.

[13] S.B. dos Reis, J. de Oliveira Silva, F. Garcia-Fossa, E.A. Leite, A. Malachias, G. Pound-Lana, V.C.F. Mosqueira, M.C. Oliveira, A.L.B. de Barros, M.B. de Jesus, Mechanistic insights into the intracellular release of doxorubicin from pH-sensitive liposomes, Biomed. Pharmacother. 134 (2021), 110952, https://doi.org/10.1016/j.biopha.2020.110952.

[14] A. Fahr, P. van Hoogevest, J. Kuntsche, M.L.S. Leigh, Lipophilic drug transfer between liposomal and biological membranes: what does it mean for parenteral and oral drug delivery? J. Liposome Res. 16 (2006) 281–301, https://doi.org/10.1080/08982100600848702.

[15] A. Hinna, F. Steiniger, S. Hupfeld, M. Brandl, J. Kuntsche, Asymmetrical flow field-flow fractionation with on-line detection for drug transfer studies: a feasibility study, Anal. Bioanal. Chem. 406 (2014) 7827–7839, https://doi.org/10.1007/s00216-014-7643-9.

[16] G. Yohannes, M. Jussila, K. Hartonen, M.L. Riekkola, Asymmetrical flow field-flow fractionation technique for separation and characterization of biopolymers and bioparticles, J. Chromatogr. A 1218 (2011) 4104–4116, https://doi.org/10.1016/j.chroma.2010.12.110.

[17] A. Bunker, T. Róg, Mechanistic understanding from molecular dynamics simulation in pharmaceutical research 1: drug delivery, Front. Mol. Biosci. 7 (2020), 604770, https://doi.org/10.3389/fmolb.2020.604770.

[18] T. Róg, M. Girych, A. Bunker, Mechanistic understanding from molecular dynamics in pharmaceutical research 2: lipid membrane in drug design, Pharmaceuticals 14 (2021) 1062, https://doi.org/10.3390/ph14101062.

[19] M. Dzieciuch, S. Rissanen, N. Szydłowska, A. Bunker, M. Kumorek, D. Jamróz, I. Vattulainen, M. Nowakowska, T. Róg, M. Kepczynski, PEGylated liposomes as carriers of hydrophobic porphyrins, J. Phys. Chem. B 119 (2015) 6646–6657, https://doi.org/10.1021/acs.jpcb.5b01351.

[20] J. Kuntsche, H. Bunjes, Influence of preparation conditions and heat treatment on the properties of supercooled smectic cholesteryl myristate nanoparticles, Eur. J. Pharm. Biopharm. 67 (2007) 612–620, https://doi.org/10.1016/j.ejpb.2007.04.019.

[21] A.B. Ormond, H.S. Freeman, Effects of substituents on the photophysical properties of symmetrical porphyrins, Dyes Pigments 96 (2013) 440–448, https://doi.org/10.1016/j.dyepig.2012.09.011.

[22] J. Lee, D.S. Patel, J. Ståhle, S.J. Park, N.R. Kern, S. Kim, J. Lee, X. Cheng, M. A. Valvano, O. Holst, Y.A. Knirel, Y. Qi, S. Jo, J.B. Klauda, G. Widmalm, W. Im, CHARMM-GUI membrane builder for complex biological membrane simulations with glycolipids and lipoglycans, J. Chem. Theory Comput. 15 (2018) 775–786, https://doi.org/10.1021/acs.jctc.8b01066.

[23] M.J. Abraham, T. Murtola, R. Schulz, S. Páll, J.C. Smith, B. Hess, E. Lindahl, GROMACS: high performance molecular simulations through multi-level parallelism from laptops to supercomputers, SoftwareX 1 (2015) 19–25, https://doi.org/10.1016/j.softx.2015.06.001.

[24] W.L. Jorgensen, J. Tirado-Rives, The OPLS [optimized potentials for liquid simulations] potential functions for proteins, energy minimizations for crystals of cyclic peptides and crambin, J. Am. Chem. Soc. 110 (1988) 1657–1666, https://doi.org/10.1021/ja00214a001.

[25] W.L. Jorgensen, J. Chandrasekhar, J.D. Madura, R.W. Impey, M.L. Klein, Comparison of simple potential functions for simulating liquid water, J. Chem. Phys. 79 (1983) 926–935, https://doi.org/10.1063/1.445869.

[26] S. Nosé, A unified formulation of the constant temperature molecular dynamics methods, J. Chem. Phys. 81 (1984) 511–519, https://doi.org/10.1063/1.447334.

[27] W.G. Hoover, Canonical dynamics: equilibrium phase-space distributions, Phys. Rev. A 31 (1985) 1695–1697, https://doi.org/10.1103/PhysRevA.31.1695.

[28] M. Parrinello, A. Rahman, Polymorphic transitions in single crystals: a new molecular dynamics method, J. Appl. Phys. 52 (1981) 7182–7190, https://doi.org/10.1063/1.328693.

[29] T. Róg, K. Murzyn, M. Pasenkiewicz-Gierula, Molecular dynamics simulations of charged and neutral lipid bilayers: treatment of electrostatic interactions, Acta Biochim. Pol. 50 (2003) 789–798.

[30] W. Humphrey, A. Dalke, K.V.M.D. Schulten, Visual molecular dynamics, J. Mol. Graph. 14 (1996) 33–38, https://doi.org/10.1016/0263-7855(96)00018-5.

[31] M. Johnsson, P. Hansson, K. Edwards, Spherical micelles and other self-assembled structures in dilute aqueous mixtures of poly(ethylene glycol) lipids, J. Phys. Chem. B 105 (2001) 8420–8430, https://doi.org/10.1021/jp011088l.

[32] OECD, Test No. 117: Partition Coefficient (n-Octanol/Water), HPLC Method, 2022. https://www.oecd-ilibrary.org/content/publication/9789264069824-en. doi: 10.3389/fmolb.2020.60A4770.

[33] H. Ibrahim, A. Kasselouri, C. You, P. Maillard, V. Rosilio, R. Pansu, P. Prognon, Meso-tetraphenyl porphyrin derivates: the effect of structural modifications on binding to DMPC liposomes and albumin, J. Photochem. Photobiol. A 217 (2011) 10–21, https://doi.org/10.1016/j.jphotochem.2010.09.008.

[34] V. Reshtov, D. Kachatkou, T. Shmigol, V. Zorin, M.A. D'Hallewin, F. Guillemin, L. Bezdetnaya, Redistribution of meta-tetra(hydroxyphenyl)chlorin (mTHPC) from conventional and PEGylated liposomes to biological substrates, Photochem. Photobiol. Sci. 10 (2011) 911–919, https://doi.org/10.1039/c0 pp00303d.

[35] S. Loew, A. Fahr, S. May, Modeling the release kinetics of poorly water-soluble drug molecules from liopsomal nanocarriers, J. Drug Del. (2011), 376548, https://doi.org/10.1155/2011/376548.

[36] P.F. Almeida, Lipid transfer between vesicles: effect of high vesicle concentration, Biophys. J. 76 (1999) 1922–1928, https://doi.org/10.1016/s0006-3495(99)77351-0.

[37] D. Tretiakova, I. Le-Deigen, N. Onishchenko, J. Kuntsche, E. Kudryashova, E. Vodovozova, Phosphatidylinositol stabilizes fluid-phase liposomes loaded with a melphalan lipophilic prodrug, Pharmaceutics 13 (2021), 473, https://doi.org/10.3390/pharmaceutics13040473.
[38] F. Ricchelli, Photophysical properties of porphyrins in biological membranes, J. Photochem. Photobiol. B 29 (1995) 109–118, https://doi.org/10.1016/1011-1344(95)07155-u.
[39] I.O.L. Bacellar, T.M. Tsubone, C. Pavani, M.S. Baptista, Photodynamic efficiency: from molecular photochemistry to cell death, Int. J. Mol. Sci. 16 (2015) 20523–20559, https://doi.org/10.3390/ijms160920523.
[40] M. Stefanelli, M. Savioli, F. Zurlo, G. Magna, S. Belviso, G. Marsico, S. Superchi, M. Venanzi, C. Di Natale, R. Paolesse, D. Monti, Porphyrins through the looking glass: spectroscopic and mechanistic insights in supramolecular chirogenesis of new self-assembled porphyrin derivates, Front. Chem. 8 (2020), 587842, https://doi.org/10.3389/fchem.2020.587842.
[41] J. Kuntsche, I. Freisleben, F. Steiniger, A. Fahr, Temoporfin-loaded liposomes: physicochemical characterization, Eur. J. Pharm. Sci. 40 (2010) 305–315, https://doi.org/10.1016/j.ejps.2010.04.005.